International Conference on Space Optics—ICSO 2006

Noordwijk, Netherlands

27–30 June 2006

Edited by Errico Armandillo, Josiane Costeraste, and Nikos Karafolas

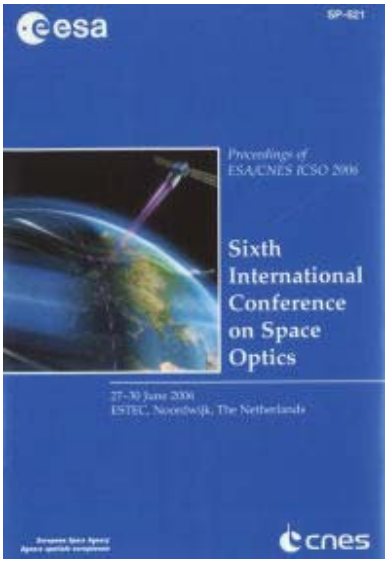

Gas-cell atomic clocks for space: new results and alternative schemes

C. Affolderbach, E. Breschi, C. Schori, G. Mileti

International Conference on Space Optics — ICSO 2006, edited by Errico Armandillo, Josiane Costeraste, Nikos Karafolas, Proc. of SPIE Vol. 10567, 105672W · © 2006 ESA and CNES
CCC code: 0277-786X/17/$18 · doi: 10.1117/12.2308185

GAS-CELL ATOMIC CLOCKS FOR SPACE: NEW RESULTS AND ALTERNATIVE SCHEMES

C. Affolderbach, E. Breschi, C. Schori, G. Mileti

Observatoire Cantonal de Neuchâtel, Rue de l'Observatoire 58, 2000 Neuchâtel, Switzerland
Email: christoph.Affolderbach@ne.ch

ABSTRACT

We present our development activities on compact Rubidium gas-cell atomic frequency standards, for use in space-borne and ground-based applications. We experimentally demonstrate a high-performance laser optically-pumped Rb clock for space applications such as telecommunications, science missions, and satellite navigation systems (e.g. GALILEO). Using a stabilised laser source and optimized gas cells, we reach clock stabilities as low as $1.5 \cdot 10^{-12}\ \tau^{-1/2}$ up to 10^3 s and $4 \cdot 10^{-14}$ at 10^4 s. The results demonstrate the feasibility of a laser-pumped Rb clock reaching $< 1 \cdot 10^{-12}\ \tau^{-1/2}$ in a compact device (<2 liters, 2 kg, 20 W), given optimization of the implemented techniques. A second activity concerns more radically miniaturized gas-cell clocks, aiming for low power consumption and a total volume around 1 cm^3, at the expense of relaxed frequency stability. Here miniaturized "chip-scale" vapour cells and use of coherent laser interrogation techniques are at the heart of the investigations.

1. INTRODUCTION

Gas-cell atomic frequency standards (often referred to as Rubidium clocks) represent a well-established type of secondary frequency references, that offers competitive frequency stabilities up to medium-term timescales (~days) in compact volumes around 0.25 to 2 liters. Industrial realizations of such clocks find applications in telecommunications, as local frequency references, and in space applications like satellite navigation systems [1, 2]. During the past years a number of studies [3, 4, 5] have been conducted on laser-pumped gas-cell frequency standards with the aim of improved frequency stability performance compared to their lamp-pumped counterparts. The narrow and precisely controllable emission spectrum of laser diodes guarantees highly efficient optical pumping, and full separation of different effects that limit the clock performance. Laser optical pumping can therefore offer superior short-term clock stabilities $\leq 3 \cdot 10^{-13}\ \tau^{-1/2}$ [3, 4], as well as high medium and long-term stabilities [5] equalling or surpassing lamp pumping technology when drifts due to thermal or light shift effects are controlled [6, 7]. It thus offers the potential to realize improved high-performance gas-cell clocks while maintaining the advantageous compact design. Here we report on the demonstration of a compact and high-performance laser-pumped Rb clock with a frequency stability reaching $1.5 \cdot 10^{-12}\ \tau^{-1/2}$ down to $< 1 \cdot 10^{-14}$ at $\tau > 10^4$ seconds, and the potential to reach a goal of $\leq 6 \cdot 10^{-13}\ \tau^{-1/2}$ and $1 \cdot 10^{-14}$ at integration times $\tau \geq 10^4$ seconds. Such frequency stabilities from an instrument with a volume ≤ 2 litres, mass ≤ 2 kg, and power consumption ≤ 20 W are of high interest for, e.g., space applications such as satellite navigation systems.

In an alternative approach, the ultimate miniaturisation of gas-cell clocks has been advanced [8], aiming for clocks with low power-consumption and 1 to 10 cm^3 volume, for use in portable end-user devices such as satellite navigation receivers, where moderate frequency stabilities around 10^{-11} over few hours are sufficient. Such clocks however require novel production techniques for miniaturized cells and mostly involve the coherent population trapping (CPT) interrogation scheme to avoid the need for a microwave cavity which inhibits to reduce the dimensions of the physics package to below the wavelength of the clock transition (≈ few centimetres). In our studies we evaluated the practical implementation of a novel excitation scheme aiming to overcome stability limitations in standard CPT clocks due to the lower signal contrast compared to the optical pumping approach [9].

2. HIGH-PERFORMANCE RB GAS-CELL CLOCKS

For the realisation of our compact high-performance clock demonstrator two main issues had to be addressed: the realization of a laser pump light source showing sufficiently good frequency and intensity stability for the short-term stability goal, and the mastering of long-term frequency drifts of the atomic reference. Such long-term drifts arise mainly from the temperature coefficient of the resonance cell and light shift effects under conditions of laser pumping; both can be controlled by fine-tuning of the cell's buffer gas content. The phase noise properties of the microwave

Proc. '6th Internat. Conf. on Space Optics', ESTEC, Noordwijk, The Netherlands, 27-30 June 2006 (ESA SP-621, June 2006)

local oscillator also affect the short-term stability, but were not addressed in this study.

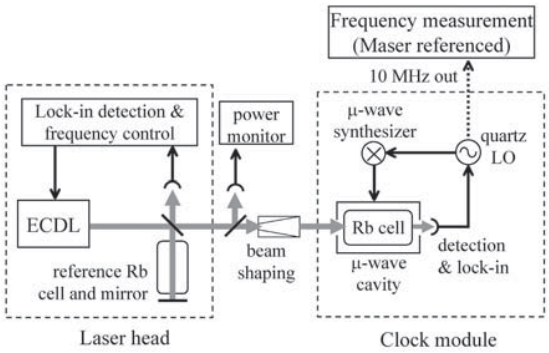

Fig. 1. Functional diagram of the laser-pumped Rb clock.

The clock is composed of a modified industrial Rb clock and a separate laser head as pump light source, while bearing in mind later integration of the laser head into the clock. The laser head contains a compact laser module and frequency stabilization to Rb absorption lines from a small reference spectroscopy setup. The laser frequency is stabilized to one of the ^{87}Rb D_2 ($5S_{1/2} \rightarrow 5P_{3/2}$) transition line components, for efficient optical pumping of the $5S_{1/2}$ ground state population of ^{87}Rb atoms contained in the clock module's resonance cell. In the clock module, the hyperfine ground-state "clock" transition at 6.8 GHz is probed by applying a microwave field to the clock cell via a microwave resonator cavity. A 10 MHz quartz local oscillator (LO) is stabilized to the center of this double-resonance signal using frequency modulation of the microwave and lock-in detection techniques (Fig. 1).

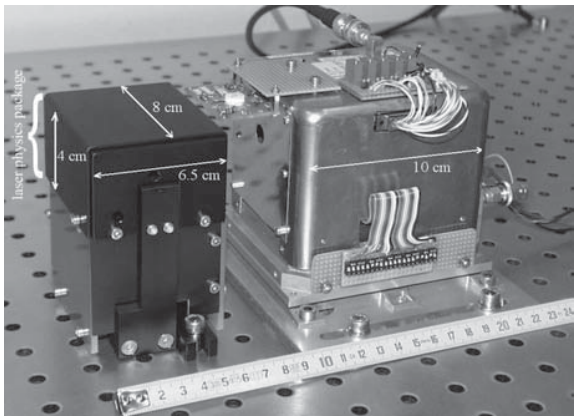

Fig. 2. Photograph of the laser-pumped Rb clock, composed of the stabilized laser head (left) and the clock module (right).

For the clock module we use an industrial Rb atomic clock (Temex Neuchâtel Time, *RAFS* type), showing lamp-pumped short-term stabilities of $3 \cdot 10^{-12}\ \tau^{-1/2}$ [2]. From this clock the discharge lamp was removed and the quartz LO was exchanged to allow for a wider tuning range during clock optimization. Furthermore, the resonance cell's buffer gas content was optimized, in order to adopt to the laser pumping conditions. Fig. 2 shows a photograph of the demonstrator clock comprised of its two sub-units.

2.1. Stabilized Laser Source

The laser head [10] has an overall physics package volume of 200 cm^3 (upper part on the left hand side in Fig. 2) and contains a compact (54 cm^3) external-cavity diode laser (ECDL) in Littrow configuration. It also includes a compact saturated-absorption set-up using a simple retro-reflected beam geometry, for laser frequency stabilization to a temperature-controlled and magnetically shielded Rb reference cell (2 cm^3 volume). The laser head emits about 2 mW of output power within a spectral width FWHM < 500 kHz. The stabilised laser has a frequency noise of 2 kHz·Hz $^{-1/2}$ and intensity noise RIN$\approx 10^{-13}$/Hz (at about 300 Hz), and shows a frequency stability of $2 \cdot 10^{-12}\ \tau^{-1/2}$ up to 100 s and $< 2 \cdot 10^{-12}$ between 10^2 and 10^5 s. These values fulfil the requirements to reach short-term clock stabilities around $2 \cdot 10^{-13}\ \tau^{-1/2}$ [3]. Passive drifts of the laser intensity amount to around $2 \cdot 10^{-4}$ at 10^4 seconds, probably due to thermal gradients and instabilities in the laser head. Here improvements can be expected from optimized thermal design, active intensity stabilization, or further miniaturization of the laser head by the implementation of advanced single-mode laser diodes such as distributed feed-back (DFB) or distributed Bragg-reflector (DBR) laser diodes. Due to the moving grating, the ECDL-based laser head shows some mechanical sensitivity, which is ideally to be avoided in an envisaged space instrument. The availability of space-worthy DFB or DBR lasers at the required wavelengths thus presents an important development issues for future space atomic clocks and other laser-based instruments.

We also evaluated a DFB laser diode emitting at 780 nm in the same laser head, by omitting the diffraction grating of the ECDL. The larger linewidth around 7 MHz of the DFB laser results in slightly increased width of the observed reference lines (≈ 30 MHz instead of ≈ 20 MHz with the ECDL), which merely degrades the short-term laser frequency stability (to around $4 \cdot 10^{-12}\ \tau^{-1/2}$) that remains compatible with the requirements for a high-performance gas-cell clock. Because the stabilisation loop acts on the DFB current only, larger drifts of the laser output power can occur than for the grating-stabilised ECDL, but these can be compensated by an additional intensity stabilisation loop acting on the laser temperature [5]. Both the ECDL-based and DFB laser head were successfully used in our Rb clock demonstrator. A detailed

characterisation of different types of diode lasers in view of their potential application to gas-cell Rb clocks can be found in [11].

2.2. Clock resonance cell properties

In this section we discuss the main relevant properties of the clock resonance cell which affect the clock stability under laser optical pumping. While the obtained signal contrast and noise levels limit the short-term frequency stability, limitations arising from the light shift are small there and become significant only for the long-term stability, as is the case for the temperature coefficient of the buffer-gas cell. We control clock instabilities arising from this temperature coefficient and the intensity-related light shift effects by choosing an appropriate mixture and absolute pressure of buffer gases for the resonance cell.

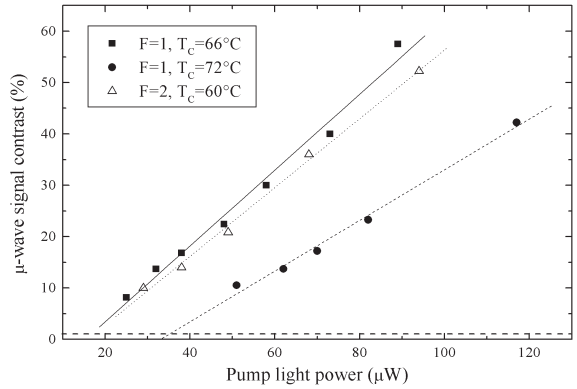

Fig. 3. Contrast of the double-resonance signal (amplitude of the resonance line divided by the dc-level out of resonance) for different cell temperatures T_C and optical pumping on the F=1 and F=2 hyperfine components. The dashed line indicates the typical signal contrast in lamp-pumped Rb clocks.

Double-resonance signal

Fig. 3 shows the double resonance signal contrast for selected cell temperatures. At typical light intensities around 30 – 60 μW/cm^2, signal contrasts around 15 to 20 % and linewidths between 0.5 and 1.5 kHz are obtained, depending on microwave power levels. This results in a higher signal-to-noise ratio and thus improved short-term clock stability compared to lamp-pumped Rb clocks, that reach typical values around 1% and 1-2 kHz respectively, at their best. From the measured double-resonance signals at the low pump light powers used, we derive a shot-noise limit for the short-term stability to be around $2\cdot10^{-13}\ \tau^{-1/2}$ [3] and an overall stability limit around $1\cdot10^{-12}\ \tau^{-1/2}$ [12]. Still better signal contrast up to 60% and thus improved short-term stability can be reached at higher light intensities or using schemes for still higher signal contrast [13]

Light Shift

The AC Stark shift or "light shift" of the clock transition induced by the pump light field constitutes a major source of instabilities in optically pumped atomic clocks [6]. As a consequence, in optically pumped gas-cell clocks the clock transition frequency f_C exhibits a dispersive shape as function of the pump light laser frequency ν_L, where the amplitude depends linearly on the total light intensity (see Fig. 4). Fluctuations of the pump light intensity or frequency will thus be translated into clock instabilities. We quantify such shifts of clock frequency due to changes in laser intensity or frequency by the proportionality parameters α (corresponding to the splitting of the light-shift curves for different light intensities) and β (slope of the light-shift curves), respectively.

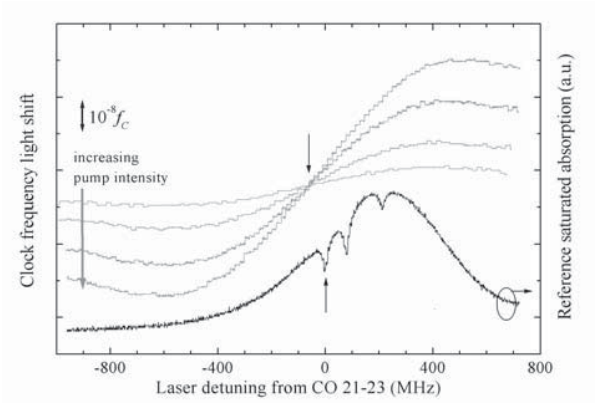

Fig. 4. Light shift of the clock frequency f_C in a lamp-optimized resonance cell for different pump light levels (10 to 65 μW/cm^2, upper 4 traces) and saturated absorption signal from the laser head's reference cell (lower trace) around the ^{87}Rb F=2 transition.

In our clock realisation we minimize the intensity light shift by precise control of the buffer gas pressure in the clock resonance cell [14], such as to make the point of $\alpha \approx 0$ (downward arrow in Fig. 4) coincide with the stabilised pump-laser frequency (upward arrow in Fig. 4), which avoids the need for active stabilization of the pump light intensity. In this approach, minimisation of the frequency-dependent light-shift parameter β is not possible at the same time, making necessary a well-stabilised pump-laser frequency. Fig. 5 shows the measured intensity related shifts of the clock frequency for different cells. For typical pump light levels (≈ 40 μW/cm^2) and with α, β expressed in fractional stability of f_C we find $\alpha \approx 2\cdot10^{-10}\ \Delta I/I$ and $\beta \approx 3\cdot10^{-17}$/Hz.

From the measured laser stability, limitations to the short-term clock stability arising from the light shift are

estimated to $\leq 1 \cdot 10^{-13}\ \tau^{-1/2}$ for both the intensity and frequency-related contributions. At 10^4 s, the measured laser intensity and frequency stabilities result in clock frequency stability limits around $4 \cdot 10^{-14}$ and $3 \cdot 10^{-14}$, respectively. Further optimisation of these limits down to around 10^{-14} at 10^4-10^5 seconds can be expected from fine adjustments of the clock cell's buffer gas content, of the pump light intensity and its fluctuations, as well as from improved laser frequency stabilization or the implementation of schemes for light shift suppression [15, 7].

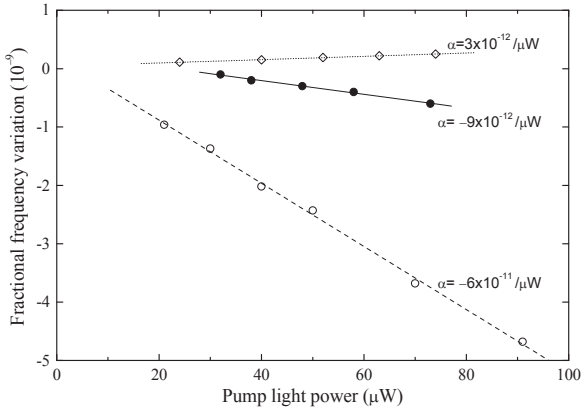

Fig. 5. Intensity-dependent light shift of the ground-state hf transition as function of the pump light power. ○: lamp-optimized cell (no.1). ●: cell no. 2 adopted for laser pumping with strongly reduced α. ◊: cell no. 3, slightly overcompensated α.

Temperature Coefficient

The use of buffer gases causes a linear shift of the atomic clock transition frequency with cell temperature, typically amounting to some 10^{-9}/K for a pure gas, which contributes to the final stability limit of the clock. In order to reduce this temperature coefficient, we thus use an appropriate mixture of two buffer gases, that cancels out the linear temperature dependence on temperature and results in a strongly reduced temperature coefficient of second order only [16]. Fig. 6 shows the measured temperature shift for the realized cell no. 2. With the cell temperature set around 57°C, the temperature coefficient is reduced to about 10^{-11}/K, resulting in a clock stability limit around 10^{-14} for cell temperature control at the millikelvin level. Refined high-precision control of the buffer gas' mixing ratio and total pressure in the cell is required in order to obtain both a low temperature coefficient at the operating cell temperature and low intensity light shift at the same time.

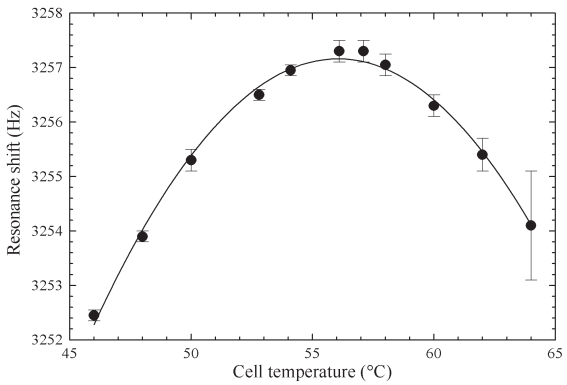

Fig. 6. Temperature dependence of the ^{87}Rb ground-state hyperfine splitting in the clock resonance cell filled with a buffer-gas mixture.

2.3. Clock Performance

The stability of the laser pumped clock was evaluated for both the laser head with the ECDL and the DFB laser implemented, and using resonance cells with a buffer gas filling adopted for laser pumping (Fig. 7). With cell no. 2 (filled circles) the temperature coefficient is greatly improved and the medium-term stability reaches $4 \cdot 10^{-14}$ at 10^4 seconds, consistent with the measured light shift coefficients and laser stability. At 10^4 seconds, the stability of our compact (≈ 2 liter, without laser electronics) clock also reproduces the performance of a much larger (≈ 27 liter) laser-pumped Cs gas-cell clock [5]. Thus our clock demonstrator today represents the most compact laser-pumped gas-cell atomic frequency standard reaching this stability level.

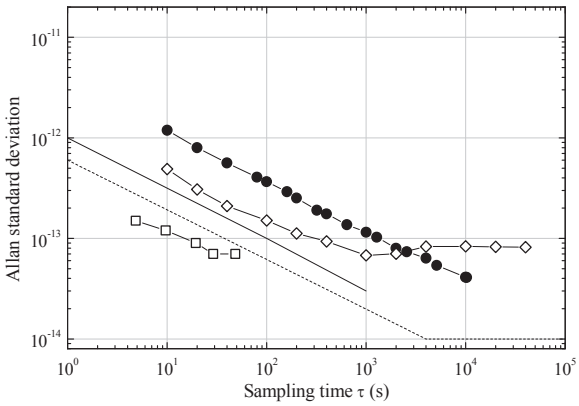

Fig. 7. Clock frequency stability performance. ●: cell no.2 with ECDL laser; ◊: cell no. 3 with DFB laser; solid line: $\sigma_y = 1 \cdot 10^{-12}\ \tau^{-1/2}$ shot noise limit; dashed line: clock performance goal; □: technology short-term stability potential as measured in [4].

Using the DFB laser head and cell no. 3 (diamonds in Fig. 7) improved short-term stability of $1.5 \cdot 10^{-12}\ \tau^{-1/2}$ is reached, while the medium-term stability is slightly degraded due to a higher temperature coefficient. Under standard laboratory conditions, the frequency drift of the clock typically lies between $2 \cdot 10^{-13}$ and $1 \cdot 10^{-12}$ /day, already comparable to or lower than those for lamp-pumped Rb clocks under the same conditions, which indicates a reduced environmental sensitivity. Continued optimization on the signal-to-noise ratio and buffer gas control is required in order to reach a state-of-the-art stability goal of $1 \cdot 10^{-14}$ over 4'000 to 10^5 seconds integration time (dashed line in Fig. 7).

3. HIGH-CONTRAST SCHEMES FOR MINIATURE ATOMIC CLOCKS

The main factor which limits the performance of CPT-based atomic clocks is the small amplitude of the CPT signal, which penalizes their short-term stability. This is largely due to the fact that the widely applied CPT interaction scheme using a two-frequency circularly polarized laser light field, has the disadvantage of putting most of the atoms into a "trap state" that does not contribute to the clock signal. In order to improve the frequency stability of CPT-based chip-scale clocks, it is thus necessary to increase the signal contrast and obtain a better signal-to-noise ratio [17]. Among other approaches, a so-called "pseudo-resonance" scheme has been proposed [18], that combines the advantages of avoiding trap states and providing low magnetic sensitivity of the reference transition. This pseudo-resonance mechanism is based on signal discrimination at the maximum of absorption between two CPT resonances. We have experimentally evaluated the potential of this scheme for improved CPT gas-cell clocks. We use a VCSEL laser diode emitting at the Rb D1 line (795 nm) and modulated at 3.4 GHz via the injection current, and obtain pseudo-resonance contrasts of up to 1.2%, compared to 5% predicted by theory for the experimental conditions ([19], see Fig. 8). With the measured detection noise levels we estimate a short-term stability limit for the atomic clock of $3 \cdot 10^{-11} \tau^{-1/2}$, to be compared to a numerically calculated shot-noise limit of $10^{-12}\ \tau^{-1/2}$. This discrepancy can be explained by the detection noise being dominated not by shot noise but by laser noise (including AM-FM conversion) and additional noise arising from the applied 3.4 GHz modulation of the laser current. In order to demonstrate the numerically predicted clock stability limits of $10^{-14}\ \tau^{-1/2}$ for this scheme under ideal conditions, not only shot-noise limited detection needs to be realised but also comparably "high-power" lasers (up to 1 mW output) with narrow (< 10 MHz) emission linewidth and sufficiently high modulation efficiency at 6.8 GHz have to be available. While these specifications are still relatively easy to obtain from an elaborate laboratory setup, their realisation within a cm-scale atomic clock presents a yet unsolved challenge that remains to be tackled.

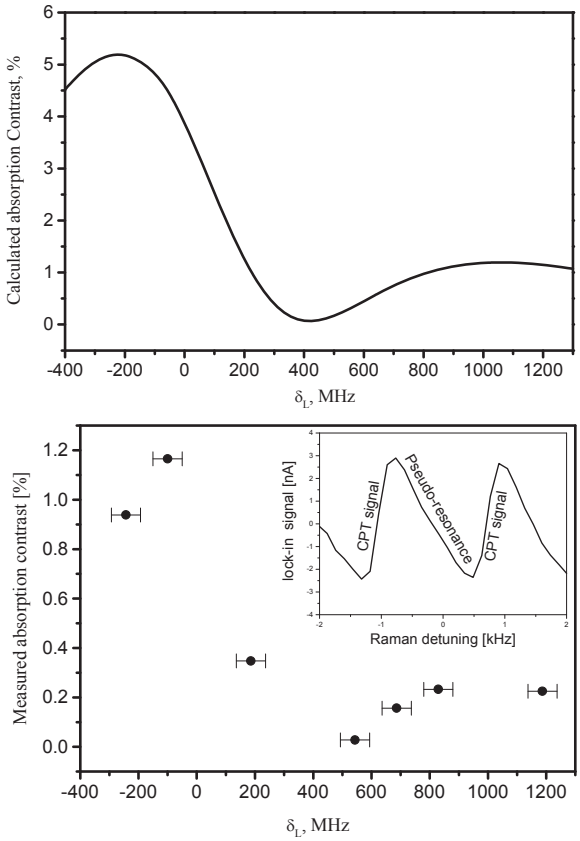

Fig. 8: Comparison of the numerically calculated (top) and experimentally measured (bottom) CPT pseudo-resonance contrast as a function of laser detuning δ_L. The inset in the bottom figure shows an example of a pseudo-resonance lock-in signal.

4. CONCLUSION

Our demonstration and evaluation of a compact laser-pumped Rb gas-cell clock underlines the potential of laser optical pumping for the realisation of state-of-the-art Rb gas-cell clocks with stabilities of 10^{-14} over few hours up to one day, while maintaining a highly compact physics package occupying a volume of less than one litre. Such frequency standards are of high interest for ground and space applications such as telecommunication or satellite navigation. Additional effort is however still needed in order to refine the key technologies involved to the required performance level, notably the refined control of buffer gas cell production, light shift control, and compact low-noise microwave sources. The availability of reliable, space-worthy, and intrinsically single-mode laser diodes (e.g.

DFB or DBR lasers) also presents a critical prerequisite for the realisation of this type of clocks and needs to be guaranteed. With the increasing availability of such suitable laser diode prototypes [11], further miniaturization of the stabilized laser source and thus of the overall clock are expected.

In the field of miniaturized "chip-scale" clocks based on CPT schemes, progress in improving the stability beyond $10^{-11}\ \tau^{-1/2}$ appears to be a challenging task. With the existing approaches for reasonably simple and compact clock realisations, this is mainly due to the typically low signal contrast and high detection noise levels, as well as to spectral limitations of the VCSEL laser diodes to be used for achieving GHz modulation. However, such cm-size clocks can still be of interest where small volume and low power consumption are required and stabilities around 10^{-10} to 10^{-11} over few hours are sufficient.

5. ACKNOWLEDGMENT

We thank Temex Neuchâtel Time SA, Ferdinand-Braun-Institut für Höchstfrequenztechnik, S. Cartaleva, C. Andreeva, D. Slavov, G. Kazakov, B. Matisov, I. Mazets, and S. Jaquet for fruitful cooperation and their contributions to the work. We acknowledge financial support by the European Space Agency (ESTEC contracts 15280/01/NL/US and 19392/05/NL/CP), the Swiss National Science Foundation (projects 200020-105624, R'Equip 2160-067498, and SCOPES VI JRPBUPJ062412 and IB7620-106115), the Canton of Neuchâtel, the Swiss Confederation (art. 16), and the Swiss University Conference (Project CIMENT).

6. REFERENCES

1. N. D. Bhaskar et al., "A historical review of atomic frequency standards used in space systems", in *Proc. 1996 IEEE Int. Frequency Control Symposium* 1996, pp. 24 – 32.

2. F. Droz et al., "On-board Galileo RAFS, current status and performances", *Proc. 2003 IEEE International Frequency Control Symposium jointly with the 17th European Frequency and Time Forum*, 2003, pp. 105 – 108.

3. G. Mileti, P. Thomann, "Study of the S/N performance of passive atomic clocks using a laser pumped vapor", in *Proc. 9th European Frequency and Time Forum*, 1995, pp. 217-276.

4. G. Mileti et al., "Laser-pumped Rubidium frequency standards: new analysis and progress", *IEEE J. Quantum Electron*., vol. 34, pp. 233 – 237, 1998.

5. Y. Ohuchi et al., "A high-stability laser-pumped Cs gas-cell frequency standard", in *Proc. IEEE International Frequency Control Symposium,* USA, 2000, pp. 651 – 655.

6. Y. Saburi et al., "Short-term stability of laser-pumped rubidium gas cell frequency standard", *Electron. Lett.*, vol. 30, pp. 633 – 635, 1994.

7. C. Affolderbach et al., "Light shift suppression in laser optically-pumped vapour-cell atomic frequency standards", *Appl. Phys. B*, vol. 80, pp. 841 - 848, 2005.

8. S. Knappe et al., "A microfabricated atomic clock", *Appl. Phys. Lett*., vol. 85, pp. 1460 – 1462, 2004.

9. R. Lutwak et al., The Chip-Scale Atomic Clock – Coherent Population Trapping vs. Conventional Interrogation, *Proc. 34th Annual Precise Time and Time Interval Systems Applications Meeting, 2002*.

10. C. Affolderbach, G. Mileti, "A compact laser head with high-frequency stability for Rb atomic clocks and optical instrumentation", *Rev. Sci. Instrum*., vol. 76, 073108, 2005.

11. D. Slavov, C. Affolderbach, G. Mileti, "Spectral characterisation of tuneable, narrow-band diode lasers for Rb atomic spectroscopy and precision instruments", in *Proc. SPIE*, vol. 5830, pp. 281 – 285, 2005.

12. C. Affolderbach, F. Droz, G. Mileti, "Experimental demonstration of a compact and high-performance laser-pumped Rubidium gas-cell atomic frequency standard", *IEEE Trans. Instrum. Meas*., vol. 55, pp. 429 – 435, 2006.

13. G. Kazakov et al., "High-contrast dark resonance on the D_2-line of ^{87}Rb in a vapor-cell with different directions of the pump-probe waves", *Eur. Phys. J. D*, vol. 35, pp. 445 – 448, 2005.

14. M. D. Rotondaro, G. P. Perram, "Collisional broadening and shift of the Rubidium D_1 and D_2 lines by rare gases, H_2, D_2, N_2, CH_4 and CF_4", *J. Quant. Spectrosc. Radiat. Transfer*, vol. 57, pp. 497 – 507, 1997.

15. J. Deng, "Light shift compensation in a Rb gas cell frequency standard with two-laser pumping", *IEEE Trans. Ultrason. Ferroel. Freq. Control*, vol. 48, pp. 1657 – 1661, 2001.

16. J. Vanier et al., "On hyperfine frequency shifts caused by buffer gases: Application to the optically pumped passive rubidium frequency standard", *J. Appl. Phys*., vol. 53, pp. 5387 – 5391, 1982.

17. M. Zhu, "High contrast signal in a coherent population trapping based atomic frequency standard application", *Proc. IEEE International Frequency Control Symposium jointly with the 17th European Frequency and Time Forum*, pp. 16-21, 2003.

18. G. Kazakov et al., "Pseudoresonance mechanism of all-optical frequency-standard operation", *Phys. Rev. A*, vol. 72, 063408 (2005).

19. G. Kazakov et al., "Evaluation of the CPT pseudo-resonance scheme for all-optical ^{87}Rb frequency standard", *Proc. 20th European Frequency and Time Forum*, 2006.